J Mater Sci: Mater Med (2007) 18:623–628
DOI 10.1007/s10856-007-2311-7

Examination of local variations in viscous, elastic, and plastic indentation responses in healing bone

Michelle L. Oyen · Ching-Chang Ko

Received: 12 January 2005 / Accepted: 13 January 2006

Abstract A viscous-elastic-plastic indentation model was used to assess the local variability of properties in healing porcine bone. Constant loading- and unloading-rate depth-sensing indentation tests were performed and properties were computed from nonlinear curve-fits of the unloading displacement-time data. Three properties were obtained from the fit: modulus (the coefficient of an elastic reversible process), hardness (the coefficient of a nonreversible, time-independent process) and viscosity (the coefficient of a non-reversible, time-dependent process). The region adjacent to the dental implant interface demonstrated a slightly depressed elastic modulus along with an increase in local time-dependence (smaller viscosity); there was no clear trend in bone hardness with respect to the implant interface. Values of the elastic modulus and calculated contact hardness were comparable to those obtained in studies utilizing traditional elastic-plastic analysis techniques. The current approach to indentation data analysis shows promise for materials with time-dependent indentation responses.

1 Introduction

Depth sensing indentation (DSI), a technique in which load and displacement are measured during a mechanical contact event, has developed into a standard technique for measurement of local properties of engineering materials. This has been due in part to the availability of commercial instruments for small-scale contact testing along with the development of a standard analytic technique for mechanical property deconvolution (the "Oliver-Pharr" method [1]). This standard technique has been used extensively and reliably for the mechanical analysis of engineering materials, including metals, glasses and ceramics, in which the response is time-independent in the experimental timeframe.

There has been recent rapid growth in small-scale DSI ("nanoindentation") analysis of biological materials, particularly calcified tissues such as bone and tooth [2–5]. Because of the capability for localized testing, nanoindentation testing is particularly well-suited to the analysis of biological materials, whose properties can vary substantially from point to point based on variations in local composition, microstructure, and cell activity. In particular, techniques which map the mechanical properties of a tissue across a biological structure show promise for understanding local structure-property linkages [6, 7]. However, the time-dependent nature of many biological materials has limited the use of DSI for testing and analysis of these tissues.

During a load-controlled nanoindentation test, creep is frequently observed in two ways: (a) increasing displacement during a holding period at fixed peak load (this hold period is a common default in commercial indentation software programs) [8] or (b) forward-displacing creep during unloading such that the maximum displacement does not occur at peak load [9]. This experimentally observed creep introduces errors when traditional elastic-plastic (Oliver-Pharr [1]) analysis of nanoindentation data is used and when time-dependence is ignored [8]. Viscoelastic models for indentation have been the focus of recent research, and in particular an analytical modeling approach exists for pyramidal

M. L. Oyen (✉)
Department of Biophysical Sciences and Medical Physics and Department of Obstetrics, Gynecology and Women's Health
e-mail: oyen0004@umn.edu, MichelleLOyen@aol.com

C.-C. Ko
Minnesota Dental Research Center for Biomaterials and Biomechanics, Department of Oral Sciences, University of Minnesota, Minneapolis, MN 55455

or conical indentation, in which viscous, elastic, and plastic deformation can all occur [9].

The purpose of the current study was to examine the variation in viscous, elastic, and plastic properties of porcine jawbone samples as a function of distance from a dental implant interface. A new unloading curve-fit technique was developed, based on the unloading solution from an existing model for time-dependent indentation originally formulated for polymeric materials [9]. Based on a previously reported gradient in elastic modulus with distance from the bone-implant interface [5] it was anticipated that the bone nearest the implant interface would have a greater time-dependent response and be softer and more compliant than bone located several millimeters from the implant interface.

2 Experimental methods

Healing bone samples adjacent to an implant interface were prepared for nanoindentation analysis in a previous study [5]. Briefly, the 4th premolars of two 2-year-old Sinclair miniswine were unilaterally removed surgically and a titanium dental implant was inserted in the alveolar ridge seven months after the extraction following procedures approved by the Animal Care and Use committee at the University of Minnesota (Protocol #9910A22661). The implants were left in place for one month prior to animal sacrifice, shielded from bite forces. Bone samples adjacent to the implant were embedded in polymer resin (PL-1, Vishay Micro-Measurements, Raleigh, NC), sectioned, and sequentially polished to 0.05 μm for indentation testing.

Indentation tests were performed using a Nanoindenter XP (MTS Systems Corp., Eden Prairie, MN) with a Berkovich pyramidal diamond indenter tip. All tests were conducted at a constant loading rate (0.333 mN s^{-1}) to a peak load of 10 mN. A total of 75 separate indentation tests on bone samples from two animals were analyzed for the current study. Spatial position was recorded for each indentation test and approximate distance from the implant interface was calculated. The load-displacement-time data for each test was exported for individual fits to the VEP (viscous-elastic-plastic) model [9]. PL-1 polymer with known elastic modulus ($E = 2.9$ GPa) and Poisson's ratio ($\nu = 0.35$)was used as a standard material to check the model implementation.

The VEP load-time ($h - t$) solution for constant loading rate indentation is

$$h_{\text{load}}(t) = \left[\frac{1}{(\alpha_2 E')^{1/2}} + \frac{1}{(\alpha_1 H)^{1/2}} + \frac{2t}{3(\alpha_3 \eta_Q)^{1/2}}\right](kt)^{1/2} \tag{1}$$

where k is the loading rate, E', H, and η_Q are the material parameters of plane strain modulus, hardness, and indentation viscosity, respectively. The numerical values of the dimensionless geometrical constants are $\alpha_3 = \alpha_2 = 4.4$, $\alpha_1 = 24.5$; [9]. (The indentation viscosity is related to an empirical time constant $\tau_Q = (\eta_Q/E)^{1/2}$ and has units Pa-s^2[9].) The plane strain (indentation) modulus E' is defined as:

$$E' = E/(1 - \nu^2) \tag{2}$$

and is equivalent to the "reduced modulus" for a rigid indenter. The VEP loading solution (Equation (1)) contains elastic and plastic deformation elements with the same functional form, and thus cannot be used in isolation to obtain independent material properties. The VEP unloading solution is

$$\begin{aligned} h_{\text{unload}} = &\left[\frac{1}{(\alpha_2 E')^{1/2}} + \frac{1}{(\alpha_1 H)^{1/2}} + \frac{2t_R}{3(\alpha_3 \eta_Q)^{1/2}}\right](kt_R)^{1/2} \\ &+ \frac{1}{(\alpha_2 E')^{1/2}}[(2kt_R - kt)^{1/2} - (kt_R)^{1/2}] \\ &- \frac{2}{3k(\alpha_3 \eta_Q)^{1/2}}\left[(2kt_R - kt)^{3/2} - (kt_R)^{3/2}\right] \end{aligned} \tag{3}$$

where t_R is the experimental rise time defined by the ratio of the peak load ($P_{\max}$) to the loading rate (k):

$$t_R = P_{\max}/k \tag{4}$$

The VEP unloading response envelops aspects of the entire indentation response: a peak point determined by viscous, elastic, and plastic deformation on loading, and an unloading response consisting of a competition between continued viscous deformation and elastic recovery. Therefore, a trial protocol was implemented to fit the experimental unloading displacement-time ($h - t$) solution to the experimental data for indentation in PL-1 polymer. The nonlinear curve-fit function in Microcal Origin 6.1 (OriginLab, Northampton, MA) was used with Levenberg-Marquardt iterations. Loading rate (k) and rise time (t_R) were fixed from the experimental input parameters. Indentation viscosity, plain strain modulus and hardness properties (η_Q, E', H) were calculated from the fits using the known geometry constants (α_i). The PL-1 plane strain modulus (E') from the model fit was 3.22 GPa, in good agreement with the calculated value of 3.30 GPa.

For indentations in bone, a Poisson's ratio of $\nu = 0.3$ was assumed [3] for calculating elastic modulus (E) from plane strain modulus (E'). Trends in property values (η_Q, E', H) with distance from the bone-implant interface were assessed by linear regression of property-distance data in transformed log coordinates.

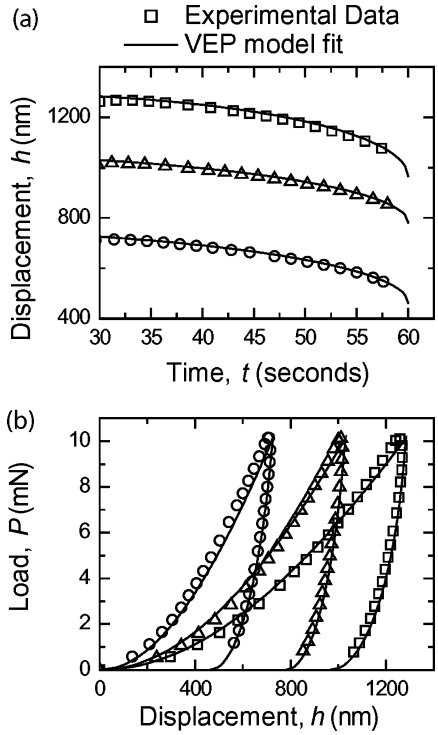

Fig. 1 (a) Displacement-time ($h - t$) traces for the unloading segment of three indentation tests on healing bone. Experimental data for three different locations on the sample are shown as open symbols; solid lines are fits to Equation (3). (b) Experimental load-displacement ($P - h$) responses for both loading and unloading responses of the same three indentation tests as above (open symbols). The solid lines were generated from the VEP model (Equations 1 and 3) using the parameters obtained in the fits in part (a).

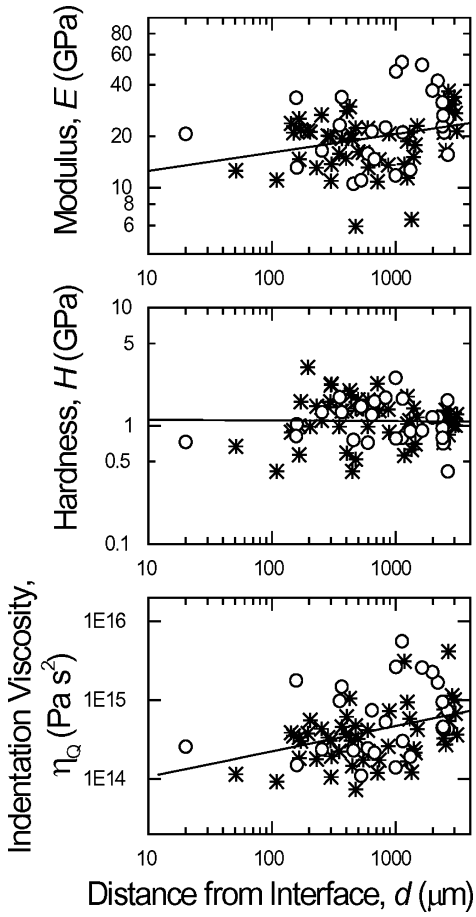

Fig. 2 VEP model fitting parameters as a function of distance d from the bone-implant interface in two porcine samples: (a) modulus E; (b) hardness H; (c) indentation viscosity η_Q. All three properties demonstrated substantial variability in both animals (individual animals shown as different symbols, o and *). Lines are fits to the data (in transformed coordinates) to indicate trends with distance from the implant interface.

Representative indentation traces for bone were constructed by inputting the mean properties (viscosity, modulus, and hardness) into the VEP model (Equations 1,3). Variation in each parameter was assessed by holding two of the three parameters fixed and varying the third parameter to the minimum and maximum values obtained in the study.

3 Results

Indentation traces for the healing bone samples demonstrated substantial point-to-point variation. Three experimental traces from the same region of the same sample are shown in Fig. 1 as open symbols. The unloading displacement-time ($h - t$) data for each curve were fit to Equation 3 and the loading response then predicted from Equation 1 based on the obtained fitting parameters. The complete VEP load-displacement ($P - h$) traces are illustrated by the solid lines in Fig. 1 (bottom), demonstrating that the experimental bone indentation data were well-described by the VEP model.

Variation in the material properties $\left(E, H, \eta_Q\right)$ is shown as a function of distance from the bone-implant interface in Fig. 2. There were variations with indent location over an order of magnitude for E and H, and over two orders of magnitude for η_Q. The average elastic modulus for all indents was 21.6 GPa. There was a trend for increasing property values with increased distance from the bone-implant interface for both E and η_Q ($p = 0.02$ and $p < 0.01$ respectively for linear regression in log coordinates), but no trend for hardness ($p = 0.893$). The indentation viscosity $\eta_Q$was found to be directly related to, and nearly a quadratic function of, the elastic modulus (power law of 1.82, Fig. 3).

The representative indentation trace for dry bone in the current study, constructed from the mean values of modulus, hardness, and viscosity, is shown as the solid line in Fig. 4. The dotted lines demonstrate the variability in indentation load-displacement response due to variations in each property; the most substantial variation in the current study was due to differences in hardness, and the least amount of variation was due to differences in viscosity.

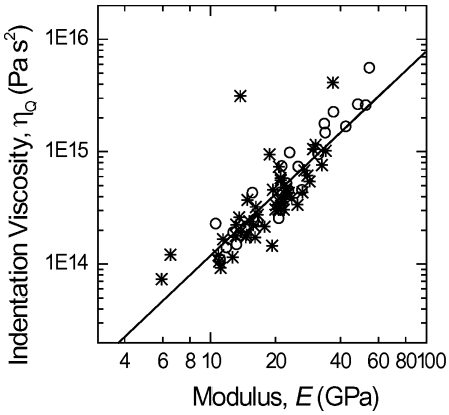

Fig. 3 Illustration of the direct dependence of VEP viscosity (η_Q) on modulus E. The relationship was nearly quadratic (power law factor 1.82)

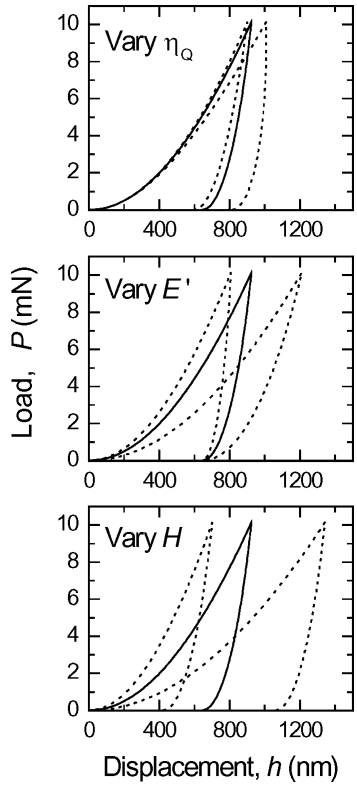

Fig. 4 Illustration of the range of indentation load-displacement ($P - h$) responses obtained in the current study. The VEP response corresponding to the average modulus (E), hardness (H), and viscosity (η_Q) terms from all samples is represented by the solid curve in each graph. Holding the other two parameters fixed, the viscosity (top), modulus (middle), and hardness (bottom) is varied over the range of values obtained from fits in the current study. The dotted lines in each plot represent the minimum and maximum values for the varied parameter.

4 Analysis and discussion

In this study, the modulus, hardness and viscosity varied substantially with indent location in samples of healing bone. The variation pattern indicates a progressive healing across the interface with immature bone (lower stiffness and viscosity) nearby the implant surface. An iterative curve fitting technique was used to calculate three different indentation properties using only the unloading displacement-time response from a constant loading- and unloading-rate indentation test. The curve-fit technique, adapted from a viscous-elastic-plastic indentation model, allowed for simple calculation of material parameters for each indentation test.

It was found in the current study that the indentation viscosity$(\eta_Q)$was not an independent parameter but was approximately proportional to the square of the elastic modulus (E). This results has interesting experimental implications, schematically illustrated in Fig. 5, in which a VEP loading- and unloading- load-displacement trace has been generated for the same hardness ($H = 0.67$ GPa), and for which a base response is compared with a response for doubled plane strain modulus ($E' = 10$ or 20 GPa) and a corresponding quadrupled viscosity ($\alpha_3\eta_Q = 5e14$ or $2e15$). The numerical values of the parameters were chosen to be representative of the results seen in the current study. As shown by the solid line approximations to the unloading stiffness (slope), the stiffness (S) is unchanged in these two cases. In frequently-used Oliver-Pharr deconvolution [1], the unloading slope (S) is used directly to calculate the plane strain modulus:

$$E' = \frac{S\sqrt{\pi}}{2\sqrt{A}} \tag{5}$$

where A is the contact area. The data shown in Fig. 5 would then lead to modulus values that would appear to differ by only a factor of 1.2 (instead of two) by Equation 5. Since the elastic stiffnesses (S) are approximately equal for the two traces shown in Fig. 5, the apparent modulus difference by Equation. (5) would be entirely due to the slightly larger contact area (A), resulting from slightly greater total displacement in the case of the $E' = 10$ GPa curve. Thus, even in the absence of an obvious viscoelastic "nose" (forward deformation on initial unloading), viscoelasitcity can substantially alter the perceived indentation mechanical properties when Oliver-Pharr analysis is used, and in this case, substantially underestimating differences between elastic modulus values.

The VEP hardness (H) is a measure of plastic deformation and is independent of elastic modulus (Fig. 6, top; $p = 0.19$ from linear regression). This parameter is not the frequently reported contact hardness (H_C) obtained from a Vickers indentation test or via the Oliver-Pharr procedure in classic nanoindentation analysis. It has been noted experimentally [3, 5] that the contact hardness is not an independent property, but scales with elastic modulus. This same observation was made by Sakai [11], who derived an analytical expression for contact hardness (H_C) in terms of the resistance to plastic deformation (H) and elastic modulus (E). This expression

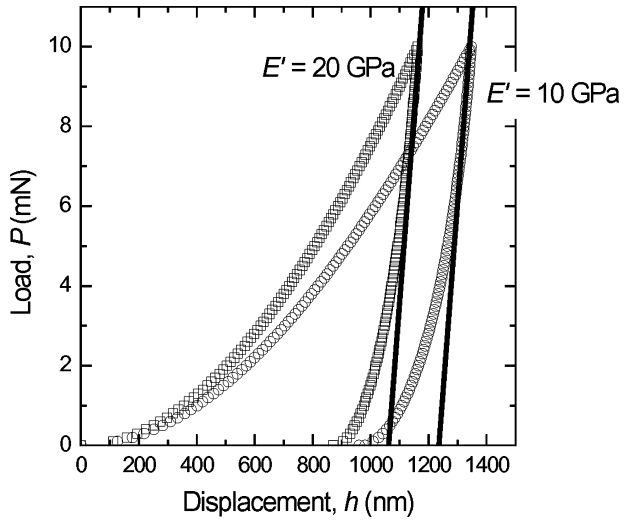

Fig. 5 Two indentation load-displacement ($P - h$) traces generated from the VEP model for plane strain modulus (E') values of 10 and 20 GPa and corresponding viscosity values based on the data shown in Fig. 3. The interactions of E and η_Q result in an apparent equivalence of the unloading stiffness S in these two responses

can be extended to include the contribution of viscous deformation, allowing the contact hardness to be calculated directly from the VEP parameters:

$$H_C = \frac{1}{\alpha_1\left((\alpha_2 E')^{-1/2} + (\alpha_1 H)^{-1/2} + (2t_R/3)(\alpha_3\eta_Q)^{-1/2}\right)^2} \tag{6}$$

For the indentation tests performed in the current study, the average contact hardness (calculated by Equation. (6) for each test) was 0.43 GPa, in good agreement with results previously reported for dry bone [2]. The calculated contact hardness increases directly with elastic modulus (Fig. 6, bottom; $p < 0.01$ from linear regression). In addition, for time-dependent materials, the measured contact hardness decreases with longer indentation test periods–either a larger rise time [9] or longer hold time at peak load [8]. One advantage to calculating the contact hardness from the E, H, t_R and η_Q values is that the infinitely fast (zero t_R) contact hardness can also be calculated and used to assess the influence of time-dependent deformation in the indentation time frame. For the current study the zero t_R contact hardness averaged 0.48 GPa. Thus, although the time-dependent deformation appeared to make a relatively small contribution to the indentation response, this mode of deformation did substantially affect the perceived contact hardness, by more than 10% in the current study.

The average elastic modulus, 21.6 GPa, was in good agreement with previously reported values for dry bone [2] even though the modulus was obtained via a different (Oliver-Pharr [1]) property deconvolution model. However, both

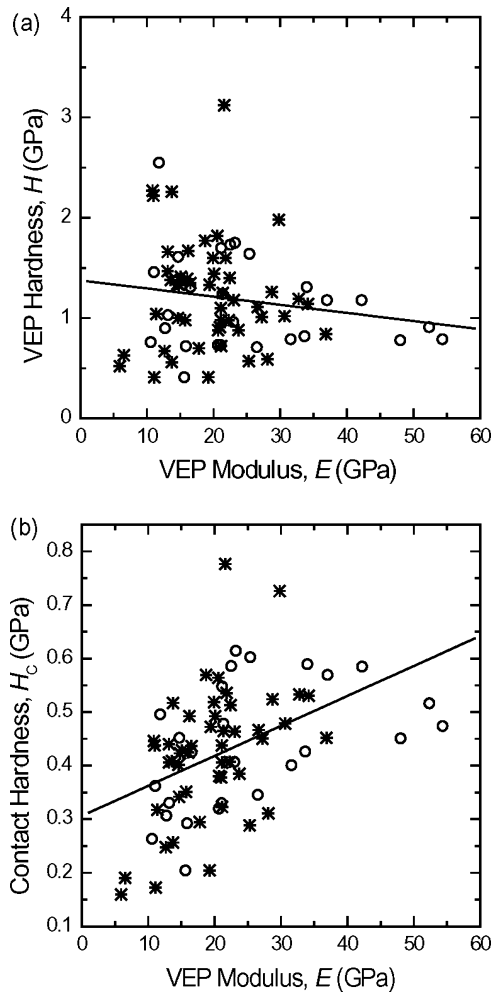

Fig. 6 (a) There is no direct relationship between the modulus (E) and hardness (H) terms obtained by VEP deconvolution of indentation load-displacement traces. (b) The calculated contact hardness (H_C, from Equation 6) increases significantly with elastic modulus

Oliver-Pharr analysis and the VEP model are based on the same elastic contact mechanics, so this agreement in elastic modulus would be anticipated. Quantitative comparison with the previous study using these same bone samples [5] showed that the numerical values of modulus in the current study were more than double those of the previous study. Some of this difference may be accounted for in that the previous study used hydrated bone while the current study tested the samples dry. The difference between wet and dry samples, reported as about 25% [2, 10], is not sufficient to explain the difference. Indenters from different manufacturers were used in the two studies, and since the frame compliance can vary with transducer design, the frame compliance value may have affected the earlier data. The polymer calibration protocol used in the previous study, which did not account for viscoelastic behavior, may also be responsible for a portion of the difference.

Both the VEP model itself and the implementation of large-scale use of the model via a fit to the unloading data

show great promise for analysis of indentation in time-dependent materials. A viscous property was reported, for the first time, along the implant-bone interface. The ability to measure this time-dependence directly by indentation is a great improvement over techniques aimed at purely removing time-dependence and measuring modulus only [8, 12]. The time-dependent property may provide important information for the study of biomechanically driven osseointegration. The quantitative nature of the model was at least partially demonstrated, in that both elastic modulus (obtained directly) and calculated contact hardness values were in good agreement with those previously reported for dry bone [2] and the trend in elastic modulus with distance from the implant interface was the same as in a prior study using the same sample set [5]. Future work will aim to extend the use of the model to materials, such as hydrated bone and soft tissues, with much smaller modulus values and much more significant time-dependent effects.

Acknowledgements This study was supported in part by the Whitaker Foundation, project RG97-0455.

References

1. W. C. OLIVER and G. M. PHARR, *J. Mater. Res.* **7** (1992) 1564.
2. J.-Y. RHO, T. Y. TSUI and G.M. PHARR, *Biomaterials* **18** (1997) 1325.
3. P. K. ZYSSET, X. E. GUO, C. E. HOFFLER, K. E. MOORE, and S. A. GOLDSTEIN, *J. Biomech.* **32** (1999) 1005.
4. E. MAHONEY, A. HOLT, M. SWAIN, and N. KILPATRICK, *J. Dent.* **28** (2000) 589.
5. M. C. CHANG, C.-C. KO, C.-C. LIU, W. H. DOUGLAS, R. DELONG, W.-J. SEONG, J. HODGES and K.-N. AN, *J. Biomech.* **36** (2003) 1209.
6. W. TESCH, N. EIDELMAN, P. ROSCHGER, F. GOLDENBERG, K. KLAUSHOFER and P. FRATZL, *Calcif Tissue Int.* **69** (2001) 147.
7. J. L. CUY, A. B. MANN, K. J. LIVI, M. F. TEAFORD, and T. P. WEIHS, *Arch. Oral. Biol.* **47** (2002) 281.
8. T. CHUDOBA and F. RICHTER, *Surface and Coatings Technology* **148** (2001) 191.
9. M. L. OYEN and R. F. COOK, *J. Mater. Res.* **18** (2003) 139.
10. A. J. BUSHBY, V. L. FERGUSON and A. BOYDE, *J. Mater. Res.* **19** (2004) 249.
11. M. SAKAI, *J. Mater. Res.* **14** (1999) 3630.
12. Z. FAN and J.-Y. RHO, *J. Biomed. Mater. Res.* **67A** (2003) 208.